Chemical synthesis and characterization of single-chain C_{18}-chloroparaffin materials with defined degrees of chlorination

Marco C. Knobloch [a,b,*], Jannik Sprengel [c], Flurin Mathis [a,d], Regula Haag [a], Susanne Kern [d], Davide Bleiner [a,b], Walter Vetter [c], Norbert V. Heeb [a]

[a] Laboratory for Advanced Analytical Technologies, Swiss Federal Institute for Materials Science and Technology Empa, Überlandstrasse 129, 8600, Dübendorf, Switzerland
[b] Department of Chemistry, University of Zürich, Winterthurerstrasse 190, 8057, Zürich, Switzerland
[c] University of Hohenheim, Institute of Food Chemistry (170b), Garbenstrasse 28, 70599, Stuttgart, Germany
[d] Zürich University of Applied Sciences ZHAW, Einsiedlerstrasse 31, 8820, Wädenswil, Switzerland

HIGHLIGHTS

- Chlorination of *n*-alkanes with SO_2Cl_2 is a versatile route to single-chain LCCPs.
- Fractionation by LC resulted in CP materials with different chlorination degrees.
- MS, NMR and elemental analysis were used to characterize synthetic C_{18}-CP mixtures.
- Proportions of olefinic and paraffinic material resemble those of SCCPs and MCCPs.
- Sulfur- and oxygen-containing side-products were identified by LC-MS.

GRAPHICAL ABSTRACT
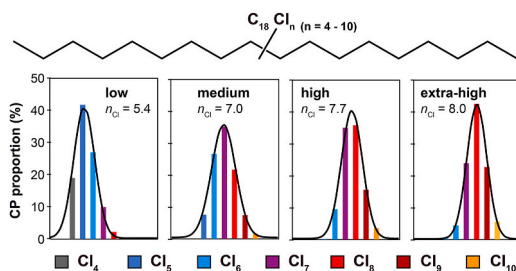
ABSTRACT

Technical chlorinated paraffins (CPs) are produced via radical chlorination of *n*-alkane feedstocks with different carbon chain-lengths (~C_{10}–C_{30}). Short-chain CPs (SCCPs, C_{10}–C_{13}) are classified as persistent organic pollutants (POPs) under the Stockholm Convention. This regulation has induced a shift to use longer-chain CPs as substitutes. Consequently, medium-chain (MCCPs, C_{14}–C_{17}) and long-chain (LCCPs, $C_{>17}$) CPs have become dominant homologues in recent environmental samples. However, no suitable LCCP-standard materials are available. Herein, we report on the chemical synthesis of single-chain C_{18}-CP-materials, starting with a pure *n*-alkane and sulfuryl chloride (SO_2Cl_2). Fractionation of the crude product by normal-phase liquid-chromatography and pooling of suitable fractions yielded in four C_{18}-CP-materials with different chlorination degrees ($m_{Cl,EA}$ = 39–52%). In addition, polar side-products, tentatively identified as sulfite-, sulfate- and *bis*-sulfate-diesters, were separated from CPs. The new single-chain materials were characterized by LC-MS, ^{1}H-NMR and EA. LC-MS provided Relative retention times for different C_{18}-CP homologues and side-products. Mathematical deconvolution of full-scan mass spectra revealed the presence of chloroparaffins (57–93%) and chloroolefins (COs, 7–26%) in the four single-chain C_{18}-CP-materials. Homologue distributions and chlorination degrees were deduced for CPs and COs. ^{1}H-NMR revealed chemical shift ranges of mono-chlorinated (δ = 3.2–5.3 ppm) and non-chlorinated (δ = 1.0–3.2 ppm) hydrocarbon moieties. The synthesized C_{18}-single-chain standard materials

---

* Corresponding author. Laboratory for Advanced Analytical Technologies, Swiss Federal Institute for Materials Science and Technology Empa, Überlandstrasse 129, 8600, Dübendorf, Switzerland.
E-mail address: marco.knobloch@empa.ch (M.C. Knobloch).

and respective spectroscopic data are useful to identify and quantify LCCPs in various materials and environmental samples. CP- and CO-distributions resemble the ones of existing SCCP and MCCP reference materials and technical mixtures. Furthermore, these materials now allow specific studies on the environmental fate and the transformation of long-chain chloroparaffins and chloroolefins.

1. Introduction

Chlorinated paraffins (CPs) are produced by UV-initiated radical chlorination from *n*-alkane mixtures (Muir et al., 2000). This process results in complex mixtures of polychlorinated paraffins with carbon chain-lengths varying from ~C_{10} to C_{30} and chlorination degrees by mass percentage m_{Cl} of 30–70% (Fiedler, 2010; Glüge et al., 2016). CPs are high production volume chemicals, produced in quantities of >1 million tons/y (Glüge et al., 2016; van Mourik et al., 2016). CPs are used as cutting fluids, plasticizers and as flame retardants (UNEP, 2016). Technical CP mixtures are complex mixtures which can contain more than 10^8 isomers (Vetter et al., 2021). In this manuscript, CPs which differ in carbon-chain length or chlorination degree are referred to as different homologues.

Short-chain CPs (SCCPs, C_{10}–C_{13}) are persistent, bioaccumulating and toxic (PBT) (Iozza et al., 2009; UNEP, 2012; Diefenbacher et al., 2015; Geng et al., 2019). As a consequence, SCCPs have been classified as persistent organic pollutants (POPs) and are regulated under the Stockholm convention since 2017 (UNEP, 2017). Because of these restrictions, SCCPs have been substituted by medium-chain CPs (MCCPs, C_{14}–C_{17}). However, MCCPs also fullfil the PBT-criteria and are currently under evaluation for restrictions (Glüge et al., 2018; ECHA, 2019; DEFRA, 2021; UNEP, 2022). This might again force the use of long-chain CPs (LCCPs, C_{18}–C_{30}). In other words, restrictions on SCCPs and MCCPs can again lead to a shift towards longer-chain CPs ($C_{\geq 18}$).

Environmental and toxicological effects of LCCPs are hardly studied (Glüge et al., 2018; Schinkel et al., 2018a; de Wit et al., 2020). Nevertheless, LCCPs have already been found in various environmental matrices and even exceed levels of SCCPs in some cases (Brandsma et al., 2017; Yuan et al., 2017; Schinkel et al., 2018a; Wang et al., 2019). In several cases, C_{18}-CPs are the most abundant LCCP-homologues (Schinkel et al., 2018a; Mézière et al., 2020a; Yuan et al., 2021). Indications were found that also LCCPs interfere with the thyroid hormone system (Sprengel et al., 2021).

LCCP-analysis is challenging. LCCPs can be identified by liquid chromatography coupled to mass selective detectors using soft ionization techniques such as electrospray (LC-ESI-MS) or atmospheric pressure chemical ionization (LC-APCI-MS) (Schinkel et al., 2018a; Mézière et al., 2020a). Under APCI conditions, CPs form negatively charged chloride-adducts $[M+Cl]^-$ in presence of dichloromethane, which minimizes fragmentation of CPs (Zencak and Oehme, 2006; Schinkel et al., 2018b; Yuan et al., 2019). Chlorination degrees derived from certain MS-methods often overestimate higher chlorinated CPs due to a higher response (Mézière et al., 2020b). Elemental analysis (EA) can deliver in general more reliable chlorination degrees if the examined CP-material does not contain impurities (Sprengel and Vetter, 2020). Nuclear magnetic resonance spectroscopy (NMR) can provide structural information about CPs (Sprengel and Vetter, 2019, 2020; Yuan et al., 2020).

Nevertheless, the identification and quantification of LCCPs with these methods is challenging because of interfered signals and the absence of reliable standard materials. Technical LCCP-mixtures with different chlorination degrees are available (type-A standards) but they usually do not match the homologue distribution of samples (Schinkel et al., 2018a; Fernandes et al., 2022). Single-chain CP-materials (type-B standards) are less complex and contain less homologues (Glüge et al., 2018). They can be used to match homologue pattern and therefore provide more reliable quantification (Tomy et al., 2000; Bogdal et al., 2015; Schinkel et al., 2018a; Mézière et al., 2020b; Fernandes et al., 2022). Single-chain CP-materials are also favorable for transformation and toxicological studies (Schinkel et al., 2018c; Heeb et al., 2019; Knobloch et al., 2021a; Zhou et al., 2021). To the best of our knowledge, single-chain LCCP standards are not yet available and we investigated their synthesis and characterization.

The UV-initiated radical chlorination of *n*-alkanes with sulfuryl chloride (SO_2Cl_2) has been used before to produce single-chain SCCPs and MCCPs (Tomy et al., 2000; Sprengel and Vetter, 2019). However, crude reaction mixtures also contained sulfite- and sulfate-diesters (Heeb et al., 2020).

Herein, we applied the sulfuryl chloride-promoted route to synthesize C_{18}-CPs. We optimized the chromatographic purification to separate CPs from side-products and could enrich CPs according to their chlorination degree. The resulting CP-fractions were combined to yield four new single-chain C_{18}-CP-materials with low, medium, high and extrahigh chlorination degrees. With this we provide a method to produce the first single-chain LCCP-materials.

These materials were characterized with LC-APCI-MS, ^{1}H-NMR and EA. CP-isotope clusters were interfered by chlorinated olefins (COs) and diolefins (CdiO). These interferences were resolved using a mathematical deconvolution procedure and proportions of paraffinic and olefinic materials were reported (Bogdal et al., 2015; Schinkel et al., 2017, 2018b; Heeb et al., 2019; Knobloch et al., 2021a).

There is some ambiguity about the chemical structures of these unsaturated materials. For example, chlorinated olefins and cyclic materials contain one double-bond equivalent (DBE). The elimination of HCl from CPs leads to COs as shown elsewhere (Schinkel et al., 2018c; Heeb et al., 2019). Assuming that the unsaturated compounds observed herein are produced by HCl-losses too, the terms chlorinated olefins (COs) and diolefins (CdiOs) are used herein for materials with one and two DBE, respectively.

Technical CP-mixtures and commercially available single-chain standard materials can contain olefinic material with variable proportions up to 28% (Li et al., 2018; Schinkel et al., 2018c; Heeb et al., 2019, 2020; Knobloch et al., 2021b; Fernandes et al., 2022). However, suppliers do not provide information on proportions of olefinic materials in these products. Such information might be important for transformation, toxicity and fate studies as well as for the quantification of CPs.

With the method presented herein, the first single-chain LCCP-materials were produced. These materials can be used as new standard materials as pointed out elsewhere (Schinkel et al., 2018a; Fernandes et al., 2022). The provided information demonstrates their suitability for the identification and quantification of C_{18}-CPs and for respective transformation, toxicological and environmental fate studies.

2. Experimental

2.1. Materials, chemicals, synthesis

A detailed procedure for the synthesis of chloroparaffins by the UV-catalyzed radical chlorination of *n*-alkanes with sulfuryl chloride (SO_2Cl_2) is described elsewhere (Sprengel and Vetter, 2019). Herein, some experimental details are briefly described. *n*-Octadecane (2 g, 7.9 mmol, purity ≥99%, Sigma-Aldrich, Buchs, Switzerland, O652-25G, Lot: MKCG6046) was dissolved in 5 mL dichloromethane (Merck, Darmstadt, Germany) and 7.5 mL sulfuryl chloride (SO_2Cl_2, Sigma Aldrich, Steinheim, Germany) was added. The reaction mixture was placed in front of a water-cooled medium-pressure mercury vapour lamp (150 W, TQ 150, Heraeus Noblelight, Hanau, Germany). After 60 min of irradiation

additional 5 mL of sulfuryl chloride were added. After additional 140 min irradiation, the reaction was quenched by transferring the mixture to 60 mL ice water. The emulsion was extracted twice with 10 mL dichloromethane at room temperature. The combined dichloromethane phases were washed with saturated sodium hydrogen carbonate solution (Roth, Karlsruhe, Germany) until a pH of 7 was achieved. The organic solvent was removed at room temperature using a gentle N_2-stream, yielding 3.96 g crude product.

2.2. Fractionation of the crude product by normal-phase liquid chromatography

The fractionation of crude synthesis product using normal-phase liquid chromatography (NP-LC) has been reported (Heeb et al., 2020) and is briefly described. Crude product (1.00 g) was loaded onto SiO_2 (65 g) in a glass column (diameter 2.5 cm). The SiO_2 was pre-heated (300 °C) and extracted with dichloromethane before usage. Fractions (F) of 20 mL solvent were collected. The solvent gradient started with *n*-hexane (F1–5) followed by mixtures of *n*-hexane and dichloromethane of 19:1 (F6–F15), 9:1 (F16–F25), 8:2 (F26–F35), 1:1 (F36–F45) and 1:9 (F46–F55). All fractions were analyzed by LC-APCI-MS as described later (chapter 2.3). CPs were found in F25 to F43, more polar side-products were detected in F43 to F57. Selected fractions, which contained pure CPs, were pooled. We produced four CP-materials of low (Cl_4–Cl_8, F25–F32), medium (Cl_4–Cl_{10}, F33–F41), high (Cl_5–Cl_{10}, F42) and extra-high (Cl_5–Cl_{10}, F43) chlorination degree. F46, F48, F50, and F52 were further used to characterize side-products. Solvents were evaporated at 30 °C and N_2-stream. After drying to constant weight, 48.0 mg of CP-material with low, 208.8 mg with medium, 63.3 with high and 240.6 mg with extra-high chlorination degree were obtained.

2.3. Mass spectrometric analysis and deconvolution of interfered mass spectra

Crude and purified CP-materials and fractions containing side-products were analyzed using a liquid chromatographic system (LC, Agilent 1290 Infinity) with a C_{18}-reverse-phase column (Agilent, SB-C18 RRHD, 50 mm × 3 mm, 1.8 μm, 50 °C) coupled to an APCI-source and a quadrupole time-of-flight mass detector (QToF-MS, Agilent 1100, Santa Clara, CA, USA). The LC-APCI-QToF-MS method has been reported before (Knobloch et al., 2021a) and is briefly described herein. Materials were dissolved in methanol to concentrations of 10 ng/μL and injected by the LC-system (6 μL). Water (A) and a mixture of methanol/dichloromethane (9/1, B) were used as eluents. The co-infusion of dichloromethane into the APCI-source leads to an enhanced formation of chloride-adduct ions $[M+Cl]^-$ (Zencak et al., 2003). Full-scan mass spectra were evaluated and chemical background was subtracted with the Mass Hunter software (B.07.00, Agilent Technologies, USA). Interferences of chloroparaffins (CPs), chloroolefins (COs) and chlorodiolefins (CdiOs) were resolved with a mathematical deconvolution procedure. A linear combination of simulated CP-, CO- and CdiO-isotope clusters is set up to represent the measured isotope cluster. Originally, the procedure has been introduced to model CP-homologue distributions (Bogdal et al., 2015; Yuan et al., 2016). As shown herein, an adopted deconvolution method can also result in non-interfered signal intensities ($I_{100\%}$) of different CP-, CO- and CdiO-homologues, which are used to calculate chlorination degrees (m_{Cl}, n_{Cl}) of respective materials (Schinkel et al., 2018b; Knobloch et al., 2021a). A scheme of the method is displayed in Figure S1. Measured and interfered isotope clusters were modeled by linear combinations of non-interfered CP-, CO- and CdiO-isotope clusters. With this procedure, proportions and non-interfered signals intensities of CPs, COs and CdiOs are obtained. Isotope clusters for deconvolution of mass spectra and identification of CPs and side-products were calculated at a mass resolution of 10′000 using EnviPat (Loos et al., 2015) and are shown in Tables S1-S6.

2.4. ^{1}H-NMR analysis

36.5 mg of the pooled, medium-chlorinated CP fractions as well as 14.2 mg of a pooled side-product fraction (F50) were measured on a NMR-instrument (300 MHz, INOVA, Varian, Palo Alto, CA, USA). ^{1}H-NMR spectra were recorded as described in a previous publication (Sprengel et al., 2019).

2.5. Elemental analysis using EA-IRMS

Elemental analysis (EA) was performed of each pooled C_{18}-CP fraction on an elemental analyzer (Euro EA 300, Eurovector, Radavalle, Italy) coupled with an IRMS (Delta plus XP system, Thermo Finnigan MAT, Bremen, Germany) with conditions described elsewhere (Vetter et al., 2012). Chlorine contents were deduced from measured carbon contents as described before (Sprengel and Vetter, 2019).

3. Results and discussion

3.1. Chromatographic characterization of synthetic single-chain C_{18}-CPs materials and side-products

Fig. 1 displays extracted ion chromatograms (EICs) of five prominent C_{18}-CP homologues (A) and side-products (B,C,D) as found in the crude synthesis product. A reverse-phase liquid chromatography (C_{18}-RP-LC) column was used to characterize and separate CPs from various polar side-products. Sulfite- (–OS(O)O–), sulfate- (-OS(O_2)O-) and bis-sulfate- (2x –OS(O_2)O-) diesters could be identified as side-products based on their characteristic isotope clusters.

Table S7 lists mean relative retention times (rrt) of different C_{18}-CP homologues and side-products. Retention times in relation to the internal standard (IS, γ-HBCD) are reported and indicated in Fig. 1. Heptachlorinated CPs were most abundant in the crude product (Fig. 1A). Mean relative retention times of tetra-, penta-, hexa-, hepta- and octachlorinated homologues gradually decreased from 1.43 to 1.39, 1.37, 1.35, 1.34 and increased again to 1.35 and 1.35 for nona- and decachlorinated CPs (Fig. 1E). In other words, homologues with lower chlorination degrees (Cl_4 to Cl_6) were partially separated, but Cl_7-to Cl_{10}-homologues with rrt of 1.34–1.35 nearly co-eluted under the given LC-conditions.

As mentioned, CPs eluted from the LC-column with rrt of 1.34–1.43, clearly after the sulfite- and sulfate-diesters, which eluted in a rrt-window of 1.11–1.19, whereas *bis*-sulfate esters eluted earliest, at rrt of 0.86–0.88 (Fig. 1E). Thus, all side-products eluted from the RP-LC column in more polar conditions than the CPs. Relative retention times, provided in Table S7, are useful to identify respective C_{18}-CP homologues and side-products.

At larger scale (1 g), CPs were fractionated by normal-phase liquid chromatography (NP-LC) on silica with a gradient of *n*-hexane/ dichloromethane mixtures (section 2.2). Overall, 60 fractions were collected and analyzed with direct-injection-CE-APCI-QToF-MS. Pure C_{18}-CP-materials were collected in fractions F25–F43, whereas fractions F44–F60 mostly contained polar side-products. Mass spectra of CP-containing fractions indicate that lower-chlorinated homologues eluted earlier from the normal-phase column than higher-chlorinated material. Due to these properies, we could gain four C_{18}-CP-materials with different chlorination degrees.

3.2. Mass spectrometric characterization of synthesized single-chain C_{18}-CP-materials

Fig. 2 displays Q-ToF mass spectra of the crude photochlorination product and four purified and pooled C_{18}-CP-materials. We used the sulfuryl chloride-mediated radical chlorination procedure to octadecane of high purity (≥99%). Nevertheless, the crude material (Fig. 2A) contains C_{18}-CPs and various sulfur- and oxygen-containing side-products.
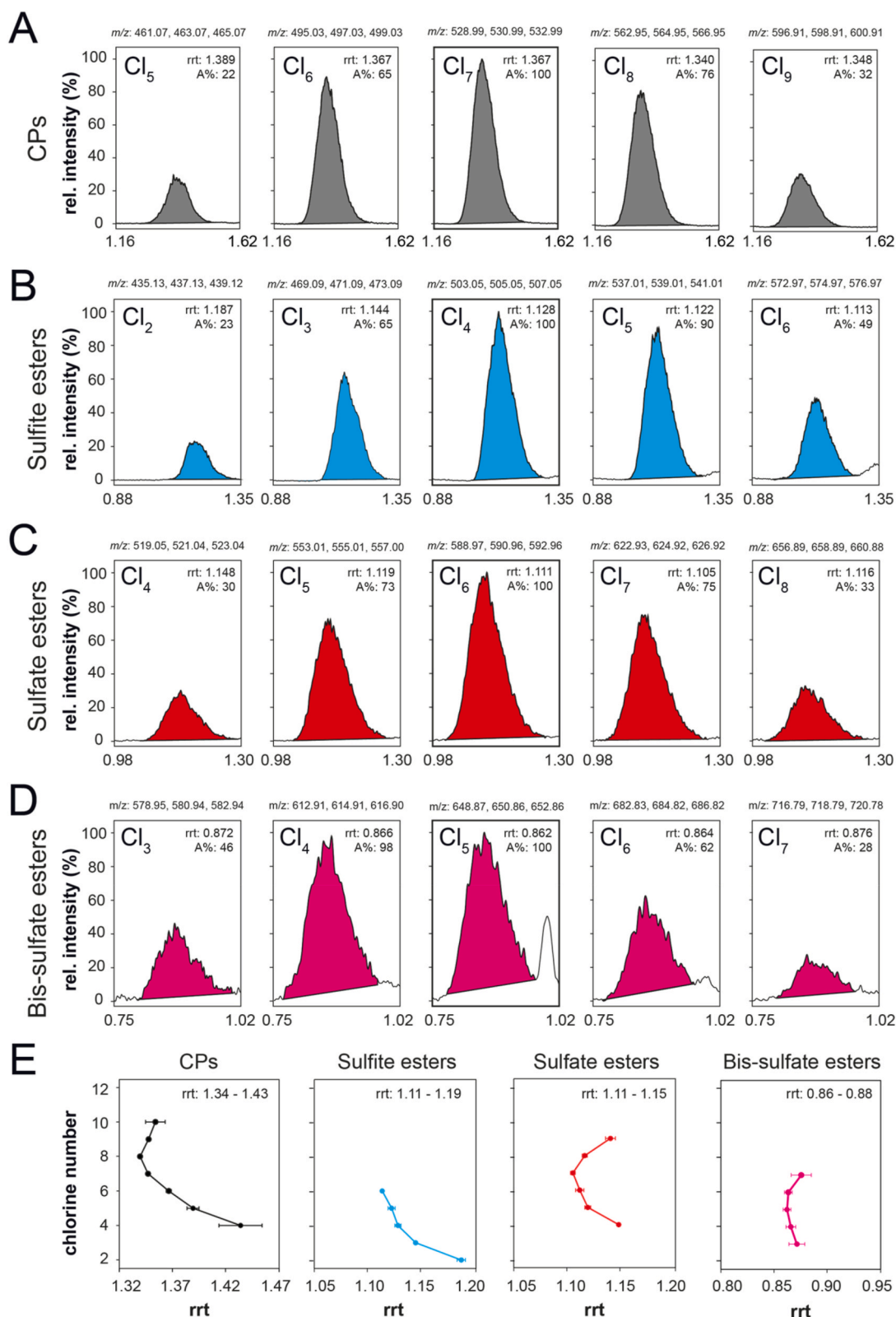
Fig. 1. LC-QToF-MS data of CPs and side-products. Extracted ion chromatograms (EIC) of three chloride-adduct ions [M+Cl]⁻ of different CP-homologues (A) and sulfur- and oxygen-containing side-products (B,C,D) are plotted. These compounds were found in the crude synthesis product and were partially separated on a C$_{18}$-reverse-phase column. Retention times (rrt) in relation to the one of the internal standard (γ-HBCD) are indicated together with the abundance (area%) in relation to the most prominent homologue (bold frame). CPs (A, gray) eluted at rrt of 1.34–1.43, more polar sulfite- (B, blue) and sulfate- (C, red) diesters between 1.11 and 1.19 and the most polar *bis*-sulfate-diesters (D, magenta) eluted at 0.86–0.88, as shown in E. (For interpretation of the references to color in this figure legend, the reader is referred to the Web version of this article.)
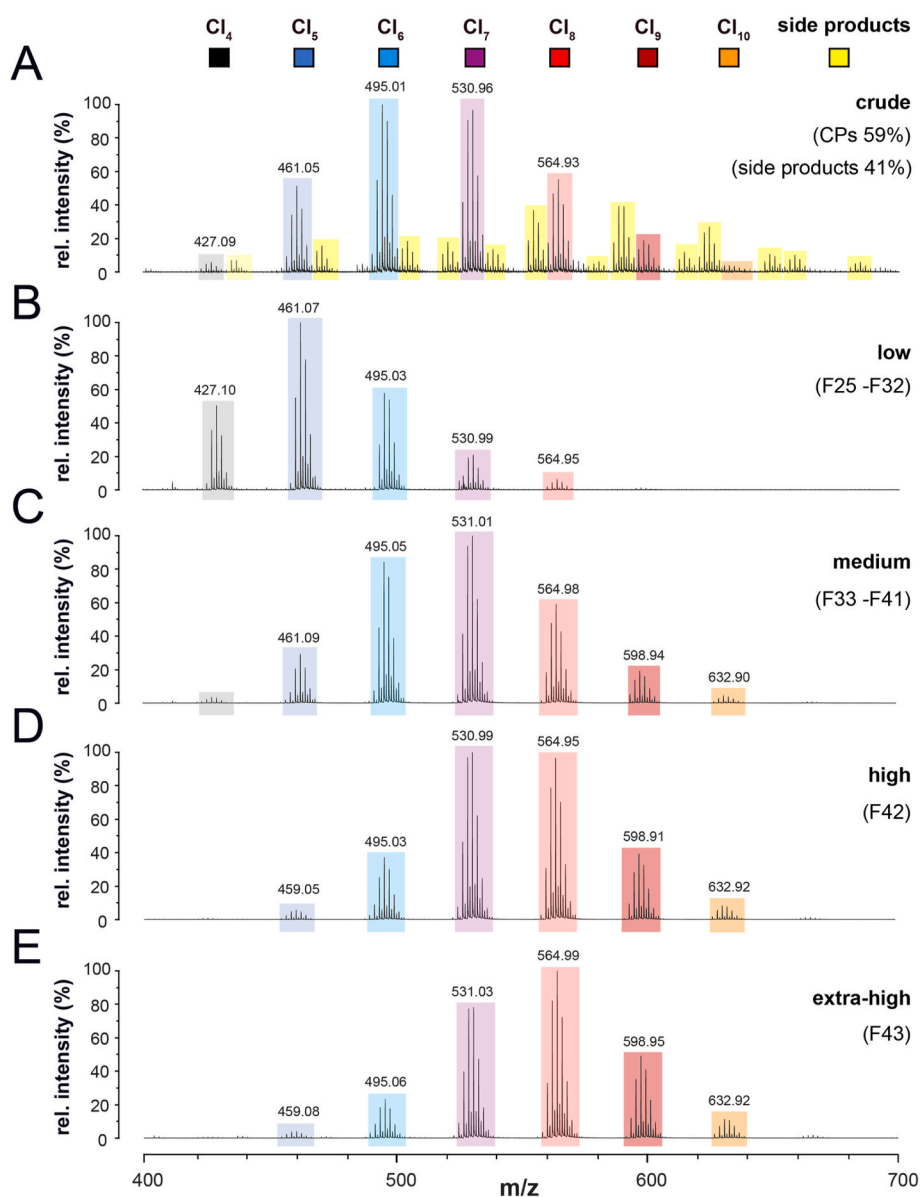
Fig. 2. QToF-mass spectra of the crude synthesis product (A) and purified (B–E) C_{18}-CP fractions of different average chlorination degrees. Chloride-adduct ions $[M+Cl]^-$ of different CP homologues are highlighted in various colors. The crude material (A) contains various polychlorinated side-products (yellow). Purification of crude material was achieved by preparative normal-phase (silica) liquid-chromatography with *n*-hexane/dichloromethane mixtures. CP-containing fractions were pooled to obtain four single-chain C_{18}-CP-materials with low (B), medium (C), high (D) and extra-high (E) chlorination degrees. No side-products could be detected in purified materials. (For interpretation of the references to color in this figure legend, the reader is referred to the Web version of this article.)

Assuming the formation of chloride-adduct ions $[M+Cl]^-$ and similar MS response of CPs and side-products, the latter would account for roughly 41% of the signal intensity of major isotope ions. This rough estimation indicates that the crude material should not be used as such for quantification and as starting materials for transformation studies.

Preparative liquid chromatography of the crude material on a normal-phase column (silica, *n*-hexane/dichloromethane mixtures) resulted in pure CP fractions (Fig. 2, F25–F43) and fractions containing polar side-products (F44–F60). CPs were partially separated on the NP-column according to their chlorination degree. We combined the pure CP-fractions in four batches and obtained four materials with different chlorination degrees. The mass spectrum of lower-chlorinated CPs which eluted first and were collected in F25–F32 is shown in Fig. 2B. F33–F41 were also combined, resulting in a material with a medium chlorination degree (Fig. 2C). Respective mass spectra of F42 and F43 which contained pure CP-materials with high and extra-high chlorination degrees are shown in Fig. 2D and E, respectively. These four purified materials with different chlorination degrees were further characterized and can be used as single-chain C_{18}-CP standard materials in transformation studies.

Different CP-homologue distributions were found in full-scan mass spectra (Fig. 2B–E). Isotope clusters of lower-chlorinated homologues, colored in gray (Cl_4) and blue (Cl_5, Cl_6) dominate in F25–F32. Higher-chlorinated homologues colored in red (Cl_8, Cl_9) and orange (Cl_{10}) are most abundant in F42 and F43. Hepta-chlorinated compounds (Cl_7) colored in violet are detected in all mass spectra.

Only C_{18}-CP homologues were detected in crude and purified materials. No indications for shorter- or longer-chain CPs were found. We conclude that no-carbon-carbon bond break occurred during radical chlorination of *n*-octadecane (purity: ≥99%). Thus, a recombination of carbon-radicals and the isomerization to non-linear C_{18}-materials is unlikely. An NMR study on single-chain MCCP-materials, which were also produced by radical chlorination with sulfuryl chloride of *n*-alkanes (Sprengel et al., 2019), did not give evidence for non-linear materials or oligomers. Thus, the herein presented materials are assumed to be linear C_{18}-CPs.

However, a detailed analysis of the different isotope clusters (Fig. 2) reveals the presence of olefinic and paraffinic materials. A mathematical deconvolution procedure was applied to resolve these interferences. Distributions of homologues and mean chlorination degrees of olefinic and paraffinic materials are discussed below. COs have been identified before and are also present in technical CP mixtures and other single-
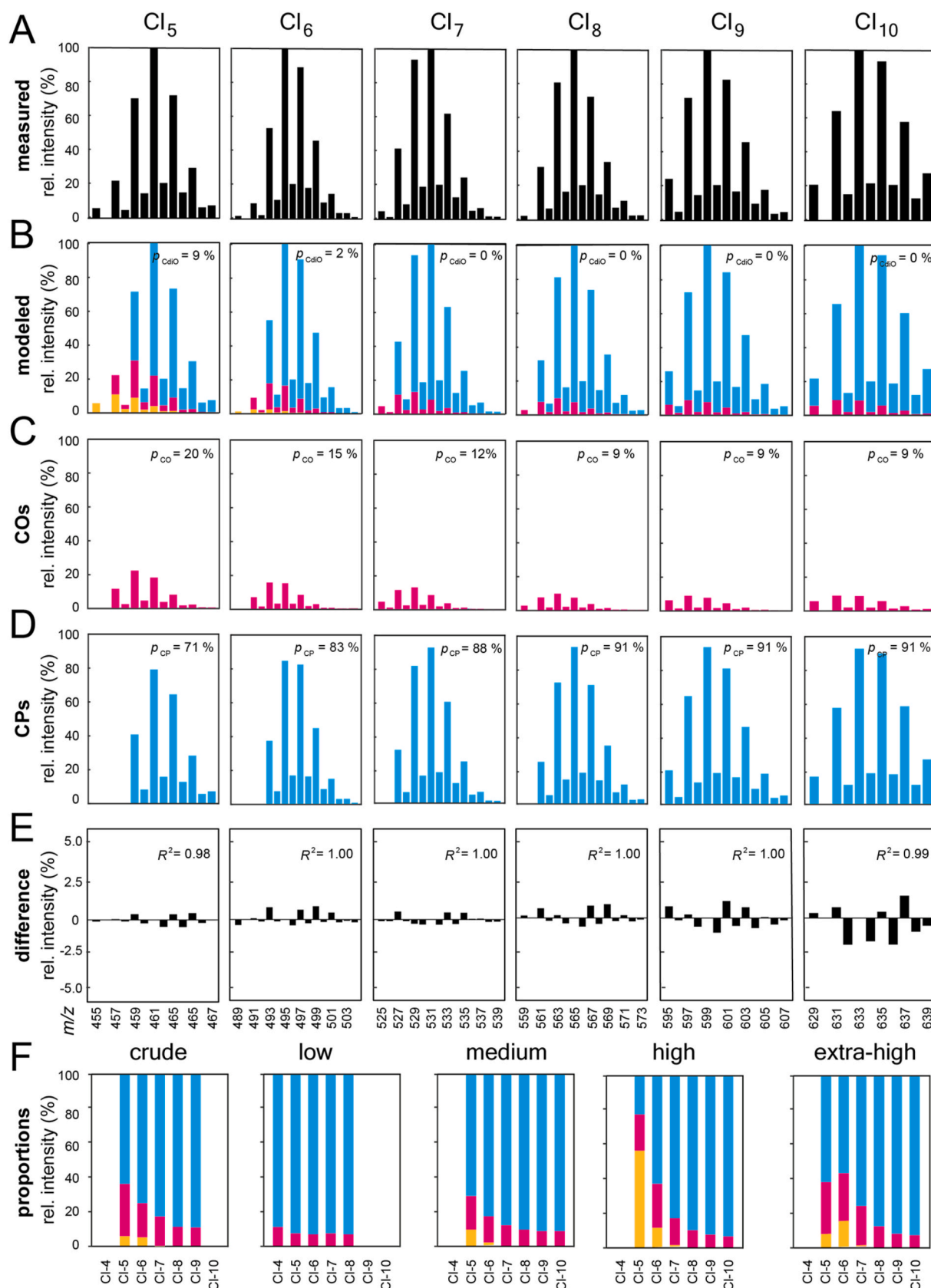
Fig. 3. Deconvolution of interfered mass spectra of the purified single-chain C_{18}-CP-material with a medium chlorination degree. Measured isotope clusters (A) are compared with modeled ones (B). Non-interfered signals of CdiOs (orange, B), COs (magenta, C) and CPs (blue, D) are displayed. Respective proportions (p_{CP}, p_{CO}, p_{CdiO}) are indicated. Differences of modeled (B) and measured (A) isotope clusters are indicated for each signal (E). The coefficients of determination R^2 of the models are displayed (E). CP-, CO- and CdiO-proportions of all homologues found in the crude and in four purified materials are compared (F). (For interpretation of the references to color in this figure legend, the reader is referred to the Web version of this article.)
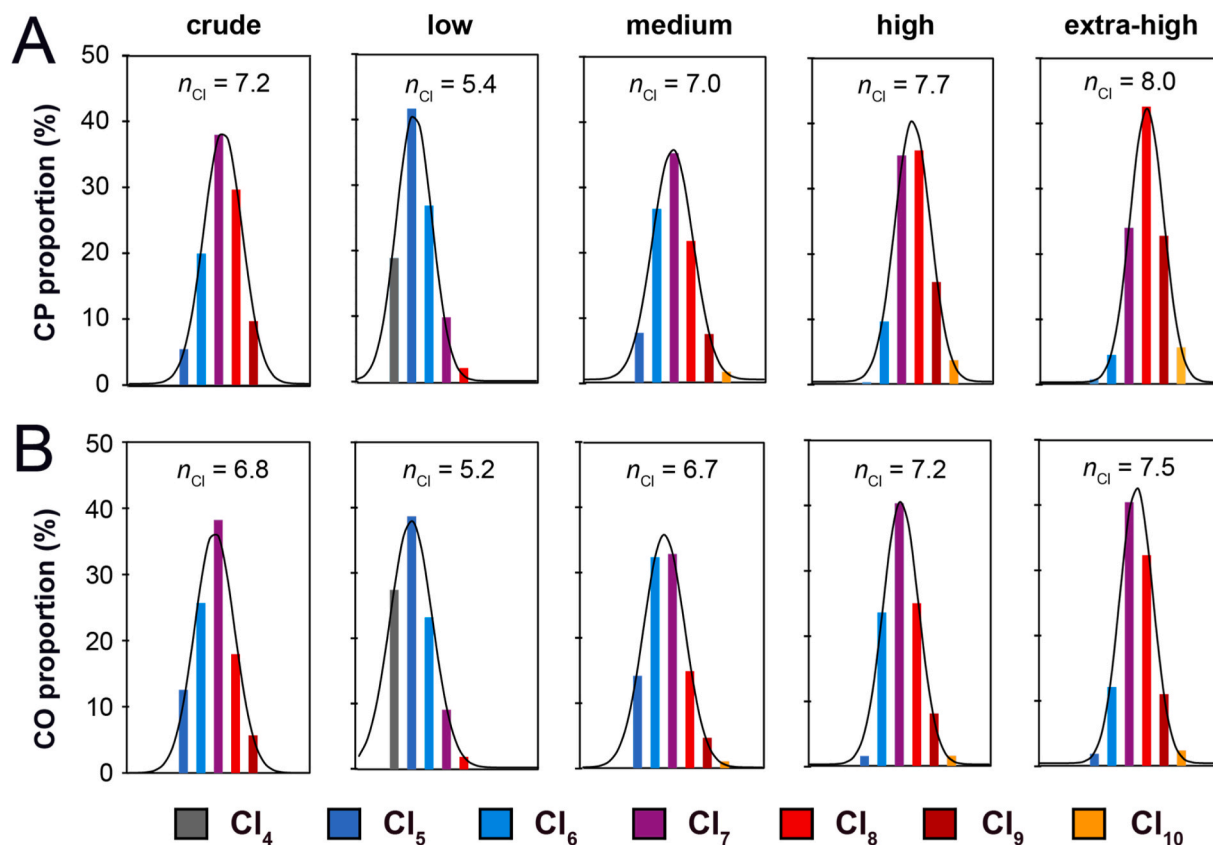
Fig. 4. Homologue distributions of paraffinic (A) and olefinic (B) C_{18}-materials. Non-interfered signal intensities ($I_{100\%}$) for different CP and CO homologues were obtained from mathematical deconvolution. From these data homologue distributions and chlorine numbers (n_{Cl}) were deduced. Respective distributions were also modeled as Gaussian functions.

chain CP-materials (Li et al., 2018; Schinkel et al., 2018c; Heeb et al., 2019; Knobloch et al., 2021b). In other words, COs seem to be ubiquitous in many CP-materials, also in the presented C_{18}-materials.

3.3. Deconvolution of paraffinic, olefinic and diolefinic material

Fig. S2 displays modeled chloride-adduct [M+Cl]⁻ isotope clusters of hexachlorinated octadecanes (Cl_6-CPs, blue, A), octadecenes (Cl_6-COs, magenta, B) and octadeca-dienes (Cl_6-CdiOs, orange, C). Overlays of the three clusters at mass resolutions of 10′000 (D,F) and 100′000 (E,G) are also given. A resolution of 10′000 is not sufficient to resolve interferences between paraffinic and olefinic C_{18}-materials. However, mathematical deconvolution (Fig. S1) enabled to determine respective proportions of CPs, COs, and CdiOs in the crude and four purified materials.

Fig. 3 gives an example of the deconvolution of interfered mass spectra of the purified C_{18}-material with a medium chlorination degree. Table S8 lists signal intensities ($I_{100\%}$) and proportions of CPs (p_{CP}), COs (p_{CO}) and CdiOs (p_{CdiO}) of the crude and purified materials as obtained from mathematical deconvolution.

The proportions of olefinic material are higher in lower-chlorinated homologues. As shown in Fig. 3C, CO proportions decreased from 20% to 9% for penta-to deca-chlorinated homologues. About 9% and 2% diolefinic material (CdiO) was found in penta- and hexachlorinated homologues (Fig. 3B). Accordingly, CP proportions increased from 71% to 91% towards higher-chlorinated homologues (Fig. 3D). In other words, CO proportions vary for different homologues and the extent of interfering ions change as well (Fig. S2). A distinction between CP-, CO- and CdiO-signals is important in order to provide accurate homologue distributions and to be able to follow transformation reactions, which lead to the formation of olefinic material. A loss of HCl, which is

associated with such transformations, has been observed before in experiments, where CPs were exposed to heat or reactive metal surfaces (Schinkel et al., 2017, 2018b, 2018b). COs are also present in commercially available single-chain materials and in industrially produced CP-mixtures (Li et al., 2018; Schinkel et al., 2018c; Heeb et al., 2019; Knobloch et al., 2021b). To the best of our knowledge, suppliers do not provide information about CO proportions in such materials. However, in transformation, toxicity and environmental fate studies CO proportions in the initial materials need to be known. The presented characterization with MS and mathematical deconvolution provides information about CO-proportions in such materials.

In general, deviations (%) from modeled and measured isotope clusters (Fig. 3E) are below 2% for abundant homologues. They can increase for homologues, which are less abundant when only few signals can be evaluated due to low signal-to-noise ratios.

It seems that the normal-phase LC-conditions, which were used to purify the crude material also effected CO-proportions to some degree (Fig. 3F). Under the given LC conditions, lower-chlorinated CPs eluted first. Respective COs were retained longer on the NP column. Thus, COs were partially enriched in later-eluting fractions (Fig. 3F). In other words, liquid chromatography, with normal- and reversed-phase columns affected homologue distributions and proportions of paraffinic and olefinic material. However, the isolation of CP- and CO-homologues remains difficult and chromatographic resolution would have to be improved considerably.

3.4. Homologue distributions of chloroparaffins and chloroolefins

Non-interfered signal intensities ($I_{100\%}$) of C_{18}-CPs, C_{18}–COs and C_{18}-CdiOs were obtained from the mathematical deconvolution procedure (Fig. S1, step H). Such data is needed to calculate chlorination degrees
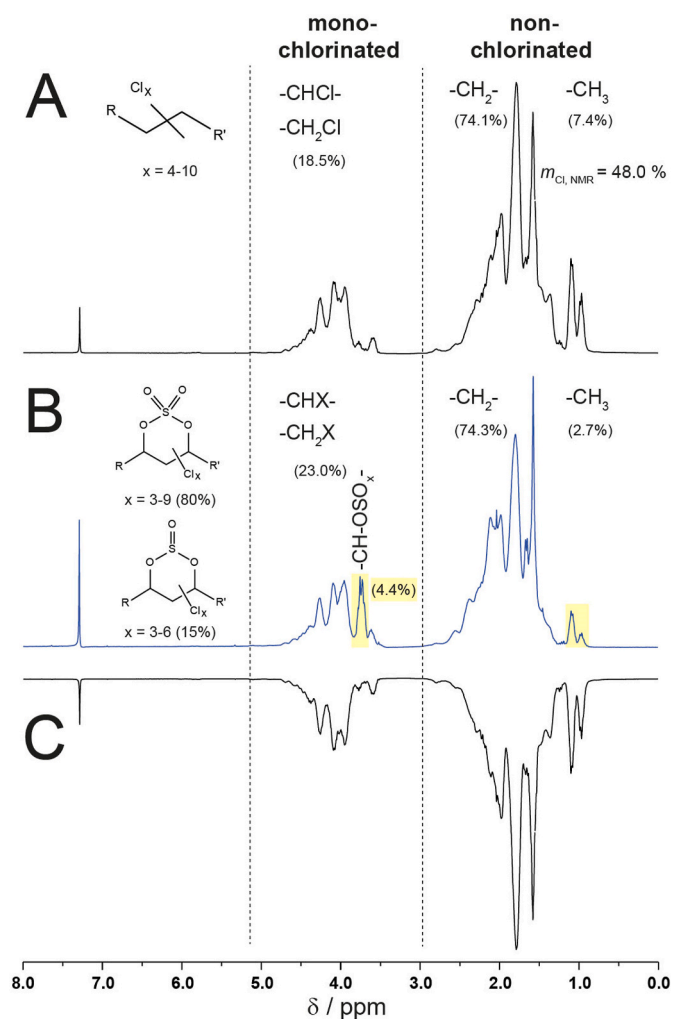
Fig. 5. ¹H-NMR spectra of a synthesized single-chain C_{18}-CP-material and of side-products. The spectrum of the purified medium-chlorinated CP-material (A, C, black) is compared with the one of F50, containing CP-sulfate- (80%) and -sulfite (15%) diesters (B, blue). Ranges of ¹H-chemical shifts (ppm) of non- and mono-chlorinated hydrocarbons are indicated (dashed lines). The CP-material (A, C) contains mainly chlorinated paraffins ($C_{18}H_{38-x}Cl_x$, x = 4–10) and some olefinic material. F50 contains mainly CP-sulfate diesters ($C_{18}H_{36-x}O_4SCl_x$, x = 4–10) and some CP-sulfite diesters ($C_{18}H_{36-x}O_3SCl_x$, x = 3–6). Molecular formulas are also provided. Signals assigned to hydrogens adjacent to sulfate- and sulfite-diesters are highlighted (B, –CH–OSO$_x$-). (For interpretation of the references to color in this figure legend, the reader is referred to the Web version of this article.)

(n_{Cl}) and homologue distributions. Fig. 4 displays CP- and CO-homologue distributions of the crude and the purified materials. C_{18}-CdiOs were neglected, because of low abundances (0–9%) in these materials. Table S9 lists mean chlorination degrees reported as chlorine numbers (n_{Cl}) and as mass percentages (m_{Cl}) both, for CPs and COs. Homologue distributions were modeled with Gaussian functions (Fig. 4).

In all cases, just four CP- or CO-homologues account for more than 90% of the distribution. Thus the chemical synthesis and the subsequent chromatography lead to comparable and rather narrow homologue distributions, which were modeled with Gaussian functions. Respective maxima varied from 35 to 42%. Peak width at half heights varied from 2.6 to 3.4.

Mean chlorine numbers (n_{Cl}) of CPs in the crude and the purified materials with low, medium, high and extra-high chlorine contents were 7.2, 5.4, 7.0, 7.7 and 8.0 (Fig. 4A). Respective values for COs were 6.8,

5.2, 6.7, 7.2 and 7.5 (Fig. 4B). In other words, chlorination degrees of CPs are always higher than those of corresponding COs. CPs can be transformed to COs with lower chlorination degree by HCl elimination. Such transformation reactions have been observed for SCCPs, which were exposed to elevated temperatures (180–220 °C) and reactive metal surfaces (Schinkel et al., 2017, 2018c, 2018c) and to certain dehalogenating enzymes (Heeb et al., 2019). From the data given in Fig. 4, we conclude that some olefinic material was also formed during the photochemical synthesis of CPs in presence of sulfuryl chloride.

The chlorination degree of the crude material is close to the one of the CP-fraction with a medium chlorine content. Earlier-eluting fractions have lower, and later-eluting fractions have higher chlorination degrees both, for CPs and COs.

In summary, the sulfuryl chloride-mediated and UV-initiated radical chlorination of octadecane ($\geq$ 99%) and subsequent NP-LC are well suited to remove polar side-products and to collect pure CP-materials with variable chlorination degrees. We received four new single-chain C_{18}-CP-materials with chlorine numbers of n_{Cl} = 5.4, 7.0, 7.7 and 8.0, corresponding to mass proportions m_{Cl} = 43.2, 50.1, 52.5 and 53.4%. Crude and medium-chlorinated materials show similar CP-homologue distributions with chlorination degrees n_{Cl} of 7.2 and 7.0. All synthesized materials also contain some COs, which could not be removed with LC. It took some efforts to deduce CP and CO proportions from interfered mass spectra for each homologue. However, because these synthetic materials will be used as precursors in environmental fate and transformation studies, it is a pre-requisite to describe their degree of saturation as well.

3.5. ¹H-NMR characterization of single-chain C_{18}-CP-materials and side-products

The chemical synthesis and subsequent preparative NP-LC resulted in mg quantities of pure single-chain C_{18}-CP-materials. An aliquot of the material with a medium chlorine content was dried at vacuum to constant mass and analyzed by ¹H-NMR (CDCl₃, 300 MHz). Fig. 5A displays the respective ¹H-NMR spectrum. Two ranges of signals can be distinguished. In the range of 3–5 ppm, hydrogens bound to mono-chlorinated carbons were observed. They accounted for 18.5% of the total signal area. Hydrogens connected to non-chlorinated carbons (~0.8–3 ppm) accounted for 81.5% of the signal area. The material contained 7.4% of non-chlorinated, terminal methyl groups (-CH₃, δ = 0.7–1.2 ppm). In other words, under the given conditions, with sulfuryl chloride as chlorine source, chlorine substitutions of hydrogens at terminal methyl groups, as well as hydrogens of methylene groups (–CH₂–) were observed. ¹H-NMR spectra of single-chain MCCP-materials and technical CP-mixtures, both produced by radical chlorination with chlorine, show similar substitution pattern (Sprengel et al., 2019; Sprengel and Vetter, 2020; Yuan et al., 2020).

Assuming that the chemical synthesis mainly resulted in chlorinated octadecanes ($C_{18}H_{38-x}Cl_x$) with small amounts of olefinic material, one can deduce a chlorine mass percentage of m_{Cl} = 48.0% from the ¹H-NMR data.

Fig. 5B displays the ¹H-NMR spectrum of those polar side-products collected in F50, which mainly contained of various sulfate- and sulfite-diesters. Respective mass spectra will be discussed later. Most ¹H-NMR-signals of the side-products (Fig. 5B, blue line) appear at comparable chemical shifts as those of the CPs (black line, mirrored). Only the proportion of terminal methyl groups (δ = 0.7–1.2 ppm) is reduced to 2.7% of the total signal area compared to 7.4% in the CP-spectrum. Furthermore, prominent signals at δ = 3.6–3.8 ppm appear, which account for 4.4% (Fig. 5B, highlighted). These signals are tentatively assigned to hydrogens adjacent to sulfate- and sulfite-diester groups (–CH–OSO$_x$-).
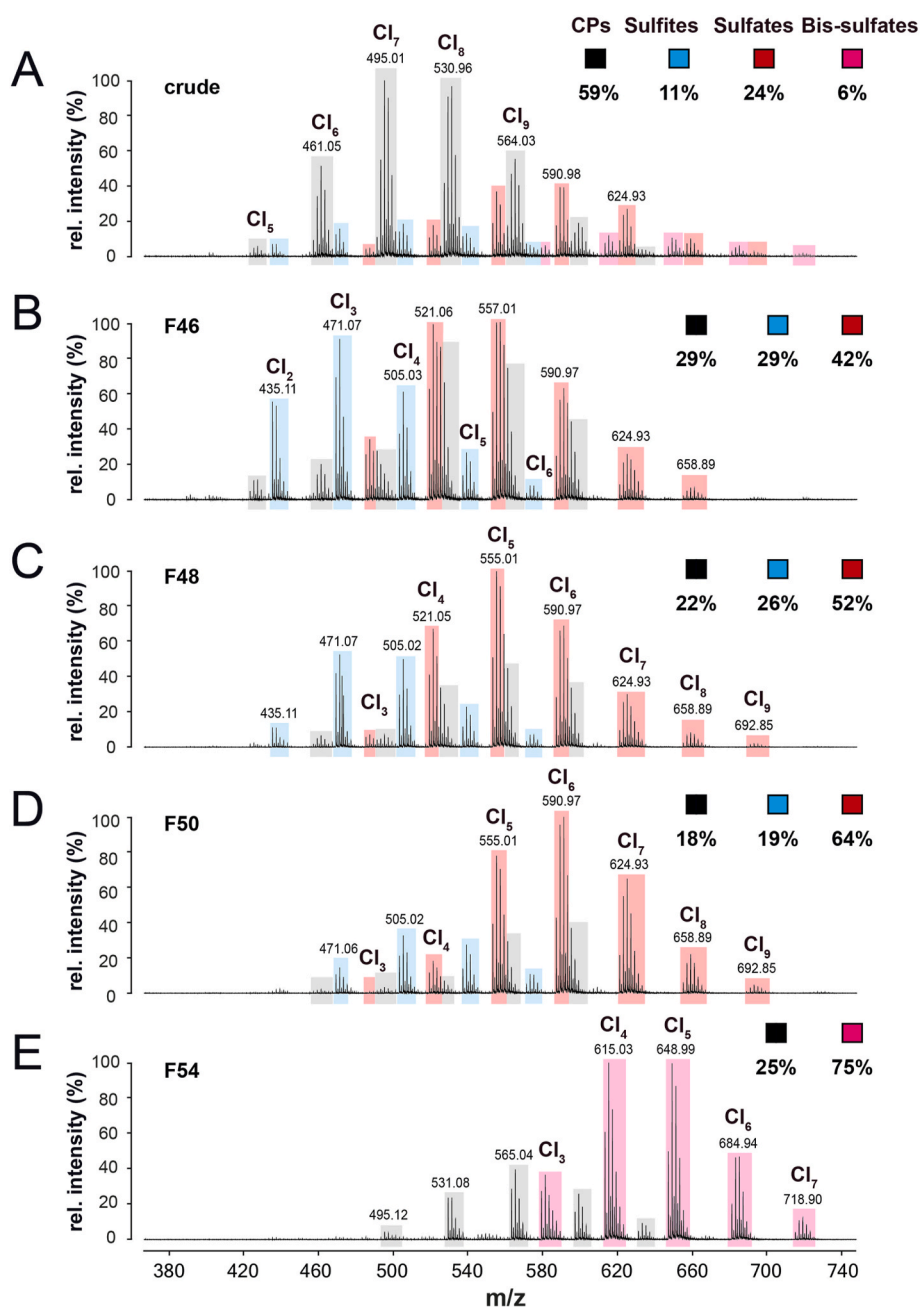
Fig. 6. LC-QToF-MS spectra of crude material (A) and selected fractions with sulfur- and oxygen-containing side-products (B–E). Chloride-adduct ions $[M+Cl]^-$ of CPs (gray), sulfite-diesters (blue), sulfate-diesters (red) and *bis*-sulfate-diesters (magenta) are highlighted. Substances were identified by comparing measured with simulated isotope clusters. Proportions of different classes of compounds were estimated under the assumption that chloride-adducts are formed in all cases with comparable MS-responses. (For interpretation of the references to color in this figure legend, the reader is referred to the Web version of this article.)

3.6. Comparison of chlorination degrees from MS-, NMR- and elemental-analysis

The chlorination degree of CP-mixtures is an important parameter and different analytical methods are in use to determine them. Chlorination degrees by mass (m_{Cl}) of the four single-chain C_{18}-CP-materials are shown in Table S9. They differ to some degree between LC-APCI-QToF-MS, ^{1}H-NMR and EA.

As discussed, CPs are the main components in the purified materials, with lower proportions of COs. It was not possible to distinguish between CPs and COs with ^{1}H-NMR and EA. Thus, chlorination degrees determined by these methods also include COs. To compare such data with QToF-MS data the chlorination degrees for CP- and CO-mixtures was calculated as well (Table S9).

Chlorination degrees (m_{Cl}) of crude and purified low, medium, high and extra-high CP-materials determined by QToF-MS were 50.4 and 43.1, 49.8, 52.1 and 53.1%. The chlorination degree of the crude

product is between those of purified materials with medium and high chlorination. Determination of (m_{Cl}) by EA of low, medium, high and extra-high chlorinated materials delivered lower values of 38.6, 47.9, 51.7 and 49.8%. ^{1}H-NMR delivered an m_{Cl} of 48.0% for medium-chlorinated material (Table S9).

Differences in chlorination degrees from EA and QToF-MS are highest for lower-chlorinated materials. LC-MS methods usually overestimate chlorination degrees of CP-mixtures due to lower response factors of lower-chlorinated homologues, as discussed elsewhere (Mézière et al., 2020b). Therefore, EA may provide more reliable chlorination degrees under the condition that pure materials are tested. However, EA cannot distinguish CPs, COs and contributions from other impurities. LC-MS can deliver good estimations of the chlorination degree for both CPs and COs and even for impurities.

Extra-high chlorinated material has the highest chlorination degree as determined by QToF-MS but not by EA. The mass spectrum of this material shows low abundances of some sulfur-containing impurities.
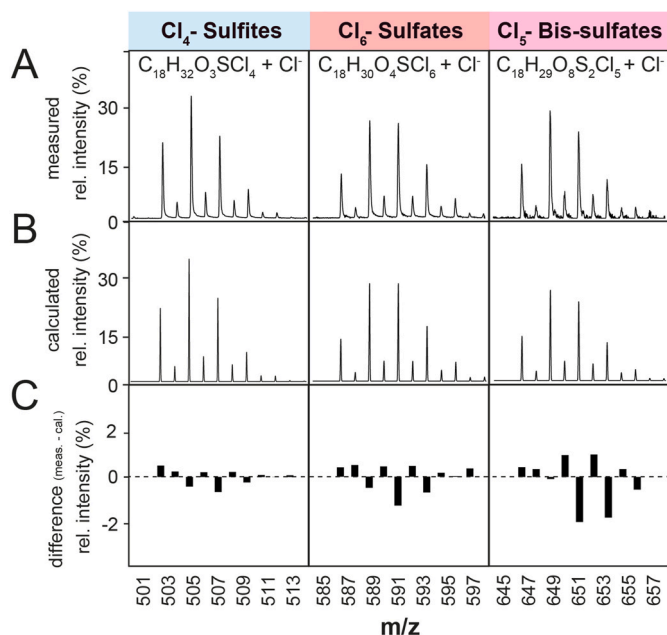
Fig. 7. Comparison of measured and calculated isotope clusters of chlorinated sulfite-, sulfate- and *bis*-sulfate-diesters. Chloride-adduct ions $[M+Cl]^-$ of measured (A) and calculated (B) isotope clusters of Cl_4-sulfites (blue), Cl_6-sulfates (red) and Cl_5-*bis*-sulfates (magenta) are compared as found in F46–F54. Differences of measured and modeled signal intensities are also shown (C). Respective formulae are also given. (For interpretation of the references to color in this figure legend, the reader is referred to the Web version of this article.)

These impurities may also lower the overall chlorination degree. The standard deviation of the EA for this material is higher too than for the other analyzed materials. The uncertainty is therefore higher as well.

We conclude that the findings of the three analytical methods are in good agreement for the purified materials with low, medium and high chlorine contents. The determined chlorination degrees m_{Cl} of the four CP-materials are in the range of technical mixtures of 30–70% (Fiedler, 2010; Glüge et al., 2016) and therefore show similar homologue distributions.

3.7. Mass spectrometric characterization of side-products

Fig. 6 shows mass spectra of the crude material (Fig. 6A) of selected fractions which contain side-products (Fig. 6B–E). Three classes of polar side-products were found in these fractions (F46, F48, F50 and F54). These side-products were tentatively assigned as series of homologues of C_{18}-sulfite- (–OS(O)O–), -sulfate (–OS(O)$_2$O–) and -*bis*-sulfate-diesters.

Assuming that these side-products form chloride-adducts as well, one can estimate proportions of different homologue series. Mass spectra show that proportions of CPs (gray) varied from 18% to 29%, those of sulfite-diesters (blue) from 19% to 29% in F46, F48 and F50, respectively (Fig. 6B, C, D). Accordingly, proportions of sulfate-diesters (red) increased in these fractions from 42 to 64%. Fraction F54 mainly contains *bis*-sulfate-diesters as polar side-products (75%) besides some CPs. Proportions of side-products in the crude material were 11, 24 and 6% for sulfite-, sulfate- and *bis*-sulfate-diesters. Cl_2-, Cl_3- and Cl_4-homologues were most abundant among the sulfites, while Cl_5-, Cl_6- and Cl_7-homologues dominated in the sulfate class.

Isotope clusters of measured and calculated C_{18}-CP-sulfite-, -sulfate- and -*bis*-sulfate-diesters are shown in Figs. S3 to S5. Fig. 7 compares measured and calculated isotope clusters of the Cl_4-sulfite-, Cl_6-sulfate- and Cl_5-*bis*-sulfate-diesters as found in F46 to F54. Measured and simulated isotope clusters agree well in all cases, with deviations of <2%. Structurally related CP-sulfate ester metabolites were identified as transformation products of SCCPs and MCCPs in rice cells (Chen et al.,

2020). This indicates that the polar, sulfur- and oxygen-containing side-products found in the synthesized material might be relevant metabolites too or can serve as potential precursors. We think that these materials are also of interest for toxicological and environmental fate studies.

However, the chemical structures of these polychlorinated sulfur- and oxygen-containing compounds are not known yet. The obtained fractions, which represent complex mixtures, might be used for further studies e.g. as precursors in toxicological tests. It is likely that sulfite- and sulfate-diesters are intermediates, which can be further transformed to CPs in photo-catalyzed reactions. Thus, we assume that these intermediates are involved in the sulfuryl chloride-induced formation of CPs.

4. Conclusions

The chemical synthesis of four single-chain C_{18}-CP-materials with defined chlorination degrees ($m_{Cl} \approx 39$–52%) could be accomplished by photochemical-chlorination of *n*-octadecane in presence of sulfuryl chloride. Preparative NP-LC of the crude synthesis product lead to various fractions of pure C_{18}-CPs. Pooling of suitable fractions allowed us to produce four C_{18}-CP-materials with different mean chlorination degrees. To the best of our knowledge, these are the first LCCP single-chain materials.

The obtained LCCP-materials were characterized by LC-MS, ^{1}H-NMR and EA. ^{1}H-NMR shows that both, terminal methyl- and internal methylene groups were chlorinated. LC-MS was used to identify and characterize polar side-products and to estimate the chlorination degrees of CPs and COs. MS-analyses revealed that COs are present in the crude as well as in purified CP-materials in abundances of 7–30%. CO-proportions in early-eluting CP-fractions were lower compared to later-eluting CP-fractions. This indicates that COs are retained longer on the NP-column compared to CPs and are enriched to some degree in later-eluting fractions.

COs are also present in commercially available single-chain materials and industrial products, in proportions up to 28% (Li et al., 2018; Schinkel et al., 2018c; Heeb et al., 2019; Knobloch et al., 2021b; Fernandes et al., 2022). However, CO-proportions are not indicated by the suppliers, but their presence can influence CP-analysis. Mass spectrometric interferences between CPs and COs can be resolved with a mass resolution of 27'000 or a mathematical deconvolution (Knobloch et al., 2021a). Only after resolving these CO- and CP-interferences, it could be shown that COs indeed are CP-transformation products formed during abiotic and biotic exposure experiments (Schinkel et al., 2018c; Heeb et al., 2019). Knowing CO levels is important for the analysis and evaluation of transformation, toxicological and fate studies of CPs.

The MS-response of CPs increases with chlorination degree. This can lead to an overestimation of the chlorination degree. Chlorination degrees deduced by ^{1}H-NMR and EA are in turn affected by the presence of COs and impurities. The crude material and the material with the highest chlorination degree (extra-high) contained some sulfur- and oxygen-containing side-products. Therefore, LC-MS shows more reliable CP-chlorination degrees for this material. We conclude that the three analytical techniques are influenced either by not resolved interferences or by differing response factors. Nevertheless, LC-MS, ^{1}H-NMR and EA all indicate similar chlorination degrees of the synthesized single-chain materials and technical mixtures and commercially available standards. This indicates that the synthesized LCCPs are appropriate standards.

Relevant amounts of polychlorinated side-products were found in the crude material and in polar fractions. Spectra of the postulated sulfite-, sulfate- and *bis*-sulfate-diesters are in accordance with the expected mass spectra. The most polar *bis*-sulfate-diesters were completely separated by normal-phase LC from the CPs and the other polar side-products, while sulfite- and sulfate-diesters could only partially be enriched in certain fractions. These fractions may be used as precursors for toxicological studies, further chemical synthesis and characterization.

C$_{18}$-CPs are abundant representatives of LCCPs and are increasingly found in environmental samples (Schinkel et al., 2018a; Mézière et al., 2020a; Yuan et al., 2021). Furthermore, the herein presented procedure can also be applied to produce other single-chain LCCP-materials.

The four obtained purified single-chain C$_{18}$-CP-materials can be used as standard materials for quantification and the provided analytical data for identification of LCCPs in various samples. Such single-chain materials are also useful to study the environmental fate and the toxicity of LCCPs.

Credit author statement

Marco C. Knobloch: Conceptualization, Methodology, Validation, Software, Data curation, Supervision, Formal analysis, Investigation, Visualization, Writing – original draft, Writing – review & editing. Jannik Sprengel: Investigation, Resources, Supervision, Visualization, Formal analysis, Writing – original draft, Writing – review & editing. Flurin Mathis: Methodology, Investigation, Validation, Data curation, Visualization, Software, Formal analysis, Visualization, Writing – original draft, Writing – review & editing. Regula Haag: Investigation, Methodology, Writing – review & editing. Susanne Kern: Supervision, Project administration, Resources, Methodology, Writing – review & editing. Davide Bleiner: Supervision, Project administration, Writing – review & editing. Walter Vetter: Conceptualization, Resources, Supervision, Writing – review & editing. Norbert V.Heeb: Conceptualization, Methodology, Validation, Data curation, Project administration, Funding acquisition, Resources, Supervision, Software, Formal analysis, Visualization, Writing – original draft, Writing – review & editing

Funding

Declaration of competing interest

The authors declare that they have no known competing financial interests or personal relationships that could have appeared to influence the work reported in this paper.

Appendix A. Supplementary data

Supplementary data to this article can be found online at https://doi.org/10.1016/j.chemosphere.2021.132938.

References

Bogdal, C., Alsberg, T., Diefenbacher, P.S., Macleod, M., Berger, U., 2015. Fast quantification of chlorinated paraffins in environmental samples by direct injection high-resolution mass spectrometry with pattern deconvolution. Anal. Chem. 87, 2852–2860. https://doi.org/10.1021/ac504444d.

Brandsma, S.H., Van Mourik, L., O'Brien, J.W., Eaglesham, G., Leonards, P.E.G., De Boer, J., Gallen, C., Mueller, J., Gaus, C., Bogdal, C., 2017. Medium-chain chlorinated paraffins (CPs) dominate in Australian sewage sludge. Environ. Sci. Technol. 51, 3364–3372. https://doi.org/10.1021/acs.est.6b05318.

Chen, W., Yu, M., Zhang, Q., Hou, X., Kong, W., Wei, L., Mao, X., Liu, J., Schnoor, J.L., Jiang, G., 2020. Metabolism of SCCPs and MCCPs in suspension rice cells based on paired mass distance (PMD) analysis. Environ. Sci. Technol. 54, 9990–9999. https://doi.org/10.1021/acs.est.0c01830.

de Wit, C.A., Bossi, R., Dietz, R., Dreyer, A., Faxneld, S., Garbus, S.E., Hellström, P., Koschorreck, J., Lohmann, N., Roos, A., Sellström, U., Sonne, C., Treu, G., Vorkamp, K., Yuan, B., Eulaers, I., 2020. Organohalogen compounds of emerging concern in Baltic Sea biota: levels, biomagnification potential and comparisons with legacy contaminants. Environ. Int. 144, 106037. https://doi.org/10.1016/j.envint.2020.106037.

DEFRA, 2021. Draft Proposal to List Chlorinated Paraffins with Carbon Chain Lengths in the Range C14-17 and Chlorination Levels ≥45% Chlorine by Weight as a Persistent Organic Pollutant (POP). Policy Pap.

Diefenbacher, P.S., Bogdal, C., Gerecke, A.C., Glüge, J., Schmid, P., Scheringer, M., Hungerbühler, K., 2015. Short-chain chlorinated paraffins in Zurich, Switzerland - atmospheric concentrations and emissions. Environ. Sci. Technol. 49, 9778–9786. https://doi.org/10.1021/acs.est.5b02153.

ECHA, 2019. Substance Evaluation Conclusion for Medium-Chain Chlorinated Paraffins/Alkanes, C14-17, Chloro. https://echa.europa.eu/de/information-on-chemicals/evaluation/community-rolling-action-plan/corap-table/-/dislist/details/0b0236e1807e3841.

Fernandes, A.R., Vetter, W., Dirks, C., van Mourik, L., Cariou, R., Sprengel, J., Heeb, N., Lentjes, A., Krätschmer, K., 2022. Determination of chlorinated paraffins (CPs): analytical conundrums and the pressing need for reliable and relevant standards. Chemosphere 286. https://doi.org/10.1016/j.chemosphere.2021.131878.

Fiedler, H., 2010. Short-chain chlorinated paraffins: production, use and international regulations. In: The Handbook of Environmental Chemistry - Chlorinated Paraffins. Springer Nature, pp. 1–40. https://doi.org/10.1007/698.

Geng, N., Ren, X., Gong, Y., Zhang, H., Wang, F., Xing, L., Cao, R., Xu, J., Gao, Y., Giesy, J.P., Chen, J., 2019. Integration of metabolomics and transcriptomics reveals short-chain chlorinated paraffin-induced hepatotoxicity in male Sprague-Dawley rat. Environ. Int. 133 https://doi.org/10.1016/j.envint.2019.105231.

Glüge, J., Wang, Z., Bogdal, C., Scheringer, M., Hungerbühler, K., 2016. Global production, use, and emission volumes of short-chain chlorinated paraffins – a minimum scenario. Sci. Total Environ. 573, 1132–1146. https://doi.org/10.1016/j.scitotenv.2016.08.105.

Glüge, J., Schinkel, L., Hungerbühler, K., Cariou, R., Bogdal, C., 2018. Environmental risks of medium-chain chlorinated paraffins (MCCPs): a review. Environ. Sci. Technol. 52, 6743–6760. https://doi.org/10.1021/acs.est.7b06459.

Heeb, N.V., Schalles, S., Lehner, S., Schinkel, L., Schilling, I., Lienemann, P., Bogdal, C., Kohler, H.P.E., 2019. Biotransformation of short-chain chlorinated paraffins (SCCPs) with LinA2: a HCH and HBCD converting bacterial dehydrohalogenase. Chemosphere 226, 744–754. https://doi.org/10.1016/j.chemosphere.2019.03.169.

Heeb, N.V., Iten, S., Schinkel, L., Knobloch, M., Sprengel, J., Lienemann, P., Bleiner, D., Vetter, W., 2020. Characterization of synthetic single-chain CP standard materials – removal of interfering side products. Chemosphere 255, 126959. https://doi.org/10.1016/j.chemosphere.2020.126959.

Iozza, S., Schmid, P., Oehme, M., Bassan, R., Belis, C., Jakobi, G., Kirchner, M., Schramm, K.-W., Kräuchi, N., Moche, W., Offenthaler, I., Weiss, P., Simoncic, P., Knoth, W., 2009. Altitude profiles of total chlorinated paraffins in humus and spruce needles from the Alps (MONARPOP). Environ. Pollut. 157, 3225–3231. https://doi.org/10.1016/j.envpol.2009.05.033.

Knobloch, M.C., Schinkel, L., Schilling, I., Kohler, H.-P.E., Lienemann, P., Bleiner, D., Heeb, N.V., 2021a. Transformation of short-chain chlorinated paraffins by the bacterial haloalkane dehalogenase LinB – formation of mono- and di-hydroxylated metabolites. Chemosphere 262, 128288. https://doi.org/10.1016/j.chemosphere.2020.128288.

Knobloch, M.C., Schinkel, L., Kohler, H.-P.E., Mathis, F., Kern, S., Bleiner, D., Heeb, N.V., 2021b. Transformation of short-chain chlorinated paraffins and olefins with the bacterial dehalogenase LinB from Sphingobium Indicum – kinetic models for the homologue-specific conversion of reactive and persistent material. Chemosphere 283, 131199. https://doi.org/10.1016/j.chemosphere.2021.131199.

Li, T., Gao, S., Ben, Y., Zhang, H., Kang, Q., Wan, Y., 2018. Screening of chlorinated paraffins and unsaturated analogues in commercial mixtures: confirmation of their occurrences in the atmosphere. Environ. Sci. Technol. 52, 1862–1870. https://doi.org/10.1021/acs.est.7b04761.

Loos, M., Gerber, C., Corona, F., Hollender, J., Singer, H., 2015. Accelerated isotope fine structure calculation using pruned transition trees. Anal. Chem. 87, 5738–5744. https://doi.org/10.1021/acs.analchem.5b00941.

Mézière, M., Cariou, R., Larvor, F., Bichon, E., Guitton, Y., Marchand, P., Dervilly, G., Bruno, L.B., 2020a. Optimized characterization of short-, medium, and long-chain chlorinated paraffins in liquid chromatography-high resolution mass spectrometry. J. Chromatogr. A 1619, 460927. https://doi.org/10.1016/j.chroma.2020.460927.

Mézière, M., Krätschmer, K., Pe Rkons, I., Zacs, D., Marchand, P., Dervilly, G., Le Bizec, B., Schächtele, A., Cariou, R., Vetter, W., 2020b. Addressing main challenges regarding short- and medium-chain chlorinated paraffin analysis using GC/ECNI-MS and LC/ESI-MS methods. J. Am. Soc. Mass Spectrom. 31, 1885–1895. https://doi.org/10.1021/jasms.0c00155.

Muir, D.C.G., Stern, G.A., Tomy, G.T., 2000. Chlorinated paraffins. In: The Handbook of Environmental Chemistry - Anthropogenic Compounds. Springer-Verlag, Berlin Heidelberg, pp. 203–236.

Schinkel, L., Lehner, S., Heeb, N.V., Lienemann, P., McNeill, K., Bogdal, C., 2017. Deconvolution of mass spectral interferences of chlorinated alkanes and their thermal degradation products: chlorinated alkenes. Anal. Chem. 89, 5923–5931. https://doi.org/10.1021/acs.analchem.7b00331.

Schinkel, L., Bogdal, C., Canonica, E., Cariou, R., Bleiner, D., McNeill, K., Heeb, N.V., 2018a. Analysis of medium-chain and long-chain chlorinated paraffins: the urgent need for more specific analytical standards. Environ. Sci. Technol. Lett. 5, 708–717. https://doi.org/10.1021/acs.estlett.8b00537.

Schinkel, L., Lehner, S., Heeb, N.V., Marchand, P., Cariou, R., McNeill, K., Bogdal, C., 2018b. Dealing with strong mass interferences of chlorinated paraffins and their transformation products: an analytical guide. TrAC Trends Anal. Chem. (Reference Ed.) 106, 116–124. https://doi.org/10.1016/j.trac.2018.07.002.

Schinkel, L., Lehner, S., Knobloch, M., Lienemann, P., Bogdal, C., McNeill, K., Heeb, N.V., 2018c. Transformation of chlorinated paraffins to olefins during metal work and thermal exposure – deconvolution of mass spectra and kinetics. Chemosphere 194, 803–811. https://doi.org/10.1016/j.chemosphere.2017.11.168.

Sprengel, J., Vetter, W., 2019. Synthesis and characterization of eight single chain length chlorinated paraffin standards and their use for quantification. Rapid Commun. Mass Spectrom. 33, 49–56. https://doi.org/10.1002/rcm.8310.

Sprengel, J., Wiedmaier-Czerny, N., Vetter, W., 2019. Characterization of single chain length chlorinated paraffin mixtures with nuclear magnetic resonance spectroscopy

(NMR). Chemosphere 228, 762–768. https://doi.org/10.1016/j. chemosphere.2019.04.094.

Sprengel, J., Vetter, W., 2020. NMR and GC/MS analysis of industrial chloroparaffin mixtures. Anal. Bioanal. Chem. 412, 4669–4679. https://doi.org/10.1007/s00216-020-02720-7.

Sprengel, J., Behnisch, P.A., Besselink, H., Brouwer, A., Vetter, W., 2021. In vitro human cell-based TTR-TRβ CALUX assay indicates thyroid hormone transport disruption of short-chain, medium-chain, and long-chain chlorinated paraffins. Arch. Toxicol. 95, 1391–1396. https://doi.org/10.1007/s00204-021-02994-5.

Tomy, G.T., Billeck, B., Stern, G.A., 2000. Synthesis, isolation and purification of C10-C13 polychloro-n- alkanes for use as standards in environmental analysis. Chemosphere 40, 679–683. https://doi.org/10.1016/S0045-6535(99)00433-6.

UNEP, 2012. Short-chained chlorinated paraffins - revised draft risk profile (UNEP/POPS/POPRC.8/6). Persistent Org. Pollut. Rev. Comm.

UNEP, 2016. Report of the Persistent Organic Pollutants Review Committee on the Work of its Twelfth Meeting. UNEP/POPS/POPRC, 12/11/Add.3 1–36.

UNEP, 2017. Decision SC-8/11 : Listing of Short-Chain Chlorinated Paraffins 14.

UNEP, 2022. Proposal to list chlorinated paraffins with carbon chain lengths in the range C14-17 and chlorination levels at or exceeding 45 percent chlorine by weight in Annexes A, B and/or C to the Stockholm Convention on Persistent Organic Pollutants. UNEP/POPS/POPRC 17/6.

van Mourik, L.M., Gaus, C., Leonards, P.E.G., de Boer, J., 2016. Chlorinated paraffins in the environment: a review on their production, fate, levels and trends between 2010 and 2015. Chemosphere 155, 415–428. https://doi.org/10.1016/j. chemosphere.2016.04.037.

Vetter, W., Kirres, J., Bendig, P., 2012. Synthesis of polychlorinated terphenyl mixtures and gas chromatography with mass spectrometry data of tetra- to octachlorinated ortho-, meta-, and para-terphenyls. J. Chromatogr. A 1263, 151–157. https://doi.org/10.1016/j.chroma.2012.09.032.

Vetter, W., Sprengel, J., Krätschmer, K., 2021. Chlorinated paraffins – a historical consideration including remarks on their complexity. Chemosphere 287, 132032. https://doi.org/10.1016/j.chemosphere.2021.132032.

Wang, H., Chang, H., Zhang, C., Wu, F., 2019. Occurrence and mass balance of medium- and long-chain chlorinated paraffins in a municipal sewage treatment plant: comparison to short-chain compounds. Environ. Int. 133, 105273. https://doi.org/10.1016/j.envint.2019.105273.

Yuan, B., Alsberg, T., Bogdal, C., MacLeod, M., Berger, U., Gao, W., Wang, Y., De Wit, C. A., 2016. Deconvolution of soft ionization mass spectra of chlorinated paraffins to resolve congener groups. Anal. Chem. 88, 8980–8988. https://doi.org/10.1021/acs. analchem.6b01172.

Yuan, B., Brüchert, V., Sobek, A., De Wit, C.A., 2017. Temporal trends of C8-C36 chlorinated paraffins in Swedish coastal sediment cores over the past 80 years. Environ. Sci. Technol. 51, 14199–14208. https://doi.org/10.1021/acs.est.7b04523.

Yuan, B., Muir, D., MacLeod, M., 2019. Methods for trace analysis of short-, medium-, and long-chain chlorinated paraffins: critical review and recommendations. Anal. Chim. Acta 1074, 16–32. https://doi.org/10.1016/j.aca.2019.02.051.

Yuan, B., Lysak, D.H., Soong, R., Haddad, A., Hisatsune, A., Moser, A., Golotvin, S., Argyropoulos, D., Simpson, A.J., Muir, D.C.G., 2020. Predicted NMR Pattern Matching Framework for Isomeric. https://doi.org/10.1021/acs.estlett.0c00244.

Yuan, B., McLachlan, M.S., Roos, A.M., Simon, M., Strid, A., de Wit, C.A., 2021. Long-chain chlorinated paraffins have reached the arctic. Environ. Sci. Technol. Lett. 8, 753–759. https://doi.org/10.1021/acs.estlett.1c00470.

Zencak, Z., Reth, M., Oehme, M., 2003. Dichloromethane-enhanced negative ion chemical ionization for the determination of polychlorinated n-alkanes. Anal. Chem. 75, 2487–2492. https://doi.org/10.1021/ac034090c.

Zencak, Z., Oehme, M., 2006. Recent developments in the analysis of chlorinated paraffins. TrAC Trends Anal. Chem. (Reference Ed.) 25, 310–317. https://doi.org/10.1016/j.trac.2005.10.005.

Zhou, Y., van Leeuwen, S.P.J., Knobloch, M., Dirks, C., Weide, Y., Bovee, T.F.H., 2021. Impurities in technical mixtures of chlorinated paraffins show AhR agonist properties as determined by the DR-CALUX bioassay. Toxicol. Vitro 72. https://doi.org/10.1016/j.tiv.2021.105098.